EPJ Web of Conferences **289**, 01008 (2023) https://doi.org/10.1051/epjconf/202328901008
*FCCP2022*

# Preparations for a search of the muon EDM at PSI

P. Schmidt-Wellenburg[1,*], C. Calzolaio[1], A. Doinaki[1], C. Dutsov[1], M. Giovannozzi[2], T. Hume[1], and F. Trillaud[3] on behalf of the muEDM collaboration.

[1] *Paul Scherrer Institute, 5232 Villigen, Switzerland*
[2] *CERN Beams Department, Esplanade des Particules 1, 1211 Meyrin, Switzerland*
[3] *Instituto de Ingeniería, Universidad Nacional Autónoma de Mexico, 04510 Ciudad de Mexico, Mexico*

**Abstract.** Electric dipole moments (EDMs) of fundamental particles violate time invariance and the combined symmetry of charge and parity (CP). The existence of a large muon EDM (muEDM) is made plausible by tensions with Standard Model predictions for semileptonic decays of heavy meson measured at LHCb, BaBar, and Belle, as well as the muon's anomalous magnetic moment (AMM). A discovery of the muEDM would manifest CP and lepton flavor universality (LFU) violation, revealing physics beyond the SM (BSM). The most sensitive muEDM search to date provides an upper limit of $1.8 \times 10^{-19}\, e{\cdot}\mathrm{cm}$ (CL 95%), extracted from high-precision data collected to measure the muon AMM. At the Paul Scherrer Institute, we are setting up a dedicated search for the muEDM using, for the first time, the frozen-spin technique to target an ultimate sensitivity better than $6 \times 10^{-23}\, e{\cdot}\mathrm{cm}$. This novel technique increases the sensitivity to EDM-induced spin precession by cancelling the AMM-induced precession with the application of a precisely tuned electric field perpendicular to the muon momentum and the magnetic field. In this configuration, the dominant source of precession is the EDM coupling to the large relativistic electric field in the muon rest frame, generated by its motion in a strong 3 T uniform magnetic field. In a precursor experiment, we will apply the frozen-spin technique in a compact solenoid demonstrating a sensitivity of better than $3 \times 10^{-21}\, e{\cdot}\mathrm{cm}$, probing uncharted and otherwise inaccessible territory in BSM theories.

## 1 Introduction

Electric dipole moments (EDMs) of fundamental particles violate time-reversal and, invoking the CPT-theorem [1], the combined symmetry of charge conjugation and parity inversion (CP). More than 70 years ago, E.M. Purcell, N.F. Ramsey and their student J.H. Smith [2] searched for an EDM of the neutron for the first time. The second search was performed using muons, measuring their longitudinal decay asymmetry after being deflected by a dipole magnet [3] resulting in an upper limit of $2.8 \times 10^{-15}\, e{\cdot}\mathrm{cm}$ (CL 95%). Since then, many searches around the world with increasing sensitivity on neutrons, atoms, and molecules [4, 5] have been concluded so far without detection.

The latest search for a muon EDM using Brookhaven National Lab's g-2 storage ring data [6], and searching for a vertical oscillation, longitudinal with respect to the main magnetic field, resulted in the current upper limit of $1.8 \times 10^{-19}\, e{\cdot}\mathrm{cm}$ (CL 95%) [7]. Using existing data from the measurements of the anomalous magnetic moment (AMM), (g-2)/2, of the muon to search for the muon EDM is economical but cannot overcome the intrinsic limitation due to the measurement of an oscillation amplitude instead of its frequency or phase. Within the historically predominant paradigm, in which lepton flavor universality and minimal flavor violation were assumed also almost universally in BSM physics, a dedicated muon EDM search did not seem attractive. It was assumed that the stringent limit on the electron EDM deduced from measurements using atoms or molecules, e.g. thorium oxide molecules $d_e < 1.1 \times 10^{-29}\, e{\cdot}\mathrm{cm}$ (CL 90%) [8], could be naively rescaled by the ratio $m_\mu/m_e$, resulting in a limit of $d_{\mu\leftarrow e} < 2.3{\times}10^{-27}\, e{\cdot}\mathrm{cm}$ (CL 90%), which is eight orders of magnitude better than the direct limit $d_\mu < 1.5 \times 10^{-19}\, e{\cdot}\mathrm{cm}$ (CL 90%). Since no new particles elucidating BSM physics have been found at the LHC yet [9, 10], the assumptions of this bygone paradigm are being relinquished. This motivates the study of flavor-violating processes and hence a direct search for the muon EDM, independent of the electron EDM limit.

When indirect effects are tested [11], high-precision measurements have access to energies that exceed the reach of the LHC. Intriguingly, the most substantial evidence for BSM appears in semileptonic B-meson decays with heavy leptons, especially with muons [12–14], at LHCb, Belle, and BaBar, violating lepton flavor universality (LFU), and in the evidence of the muon g-2 discrepancy with SM expectations [15, 16]. These striking hints for new physics are incompatible with minimal flavor violation (MFV) in the lepton sector [17]. In effective-field theories, the imaginary part of the Wilson coefficient, of

* e-mail: $\mu$philipp.schmidt-wellenburg@psi.ch

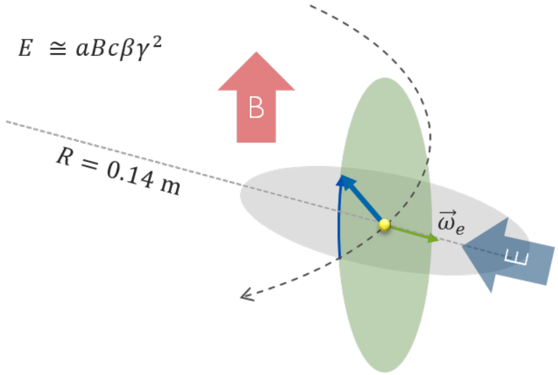


**Figure 1.** Illustration of the spin precession due to the AMM and the EDM of the muon.

which the real part gives rise to the g-2 of a lepton, also gives rise to the EDM [18, 19]. This intrinsic connection of the EDM to the g-2 and the tantalising evidence for LFU violation can only be tested by a dedicated high-sensitivity search for the muon EDM.

## 2 The frozen-spin technique in a compact solenoid

The EDM of a charged particle with charge $q$ and spin $\hbar/2$, $\vec{s}$, can be described as $\vec{d} = \eta q\vec{s}/(2mc)$ and leads to a two-fold energy splitting when exposed to an electric field with

$$\Delta E = 2\vec{d} \cdot \vec{E}, \tag{1}$$

corresponding to a transition frequency between the upper and lower energy states of $\omega_e = 2d|E|/\hbar$. As the spin is an axial vector while the electric field is a vector, the scalar product of the two violates time and parity symmetry, and by the CPT theorem [1] also the combined symmetry of charge conjugation and parity (CP).

The spin dynamics of a charged particle with spin $\hbar/2$ in a magnetic and electric field is described by the Thomas-Bargman, Michel, and Telegdi [20, 21] equation,

$$\begin{aligned}\vec{\omega}_a &= \vec{\omega}_c - \vec{\omega}_0 \\ &= -\frac{q}{m}\left[a\vec{B} - \frac{a\gamma}{(\gamma+1)}\left(\vec{\beta}\cdot\vec{B}\right)\vec{\beta} - \left(a + \frac{1}{1-\gamma^2}\right)\frac{\vec{\beta}\times\vec{E}}{c}\right],\end{aligned} \tag{2}$$

where $\vec{\omega}_c$ and $\vec{\omega}_0$ are the relativistic cyclotron and Larmor frequency, respectively and $a = (g-2)/2$ is the anomalous magnetic moment. This will result in a precession of the spin aligned with the magnetic field, $\vec{\omega} \parallel \vec{B}$, indicated by the gray ellipse in Fig. 1.

An EDM $\vec{d}$ will result in an additional oscillation,

$$\vec{\omega}_e = \frac{\eta q}{2m}\left[\vec{\beta}\times\vec{B} + \frac{\vec{E}}{c} - \frac{\gamma c}{(\gamma+1)}\left(\vec{\beta}\cdot\vec{E}\right)\vec{\beta}\right], \tag{3}$$

perpendicular to momentum and magnetic field. To employ the frozen-spin technique, the electric field must be tuned so that

| | phase I | phase II |
|---|---|---|
| Muon flux ($\mu^+/s$) | $4 \times 10^6$ | $1.2 \times 10^8$ |
| Channel transmission | 0.03 | 0.005 |
| Injection efficiency | 0.017 | 0.60 |
| Muon storage rate (1/s) | $2 \times 10^3$ | $360 \times 10^3$ |
| Gamma factor $\gamma$ | 1.04 | 1.56 |
| Magnetic field (T) | 3 | 3 |
| Electric field (kV/cm) | 3 | 20 |
| $e^+$ detection rate (1/s) | 500 | $90 \times 10^3$ |
| **Detections per 200 days** | $8.64 \times 10^9$ | $1.5 \times 10^{12}$ |
| Mean decay asymmetry | 0.3 | 0.3 |
| Initial polarization $P_0$ | 0.95 | 0.95 |
| **Sensitivity** ($e\cdot$cm) | $< 3 \times 10^{-21}$ | $< 6 \times 10^{-23}$ |

**Table 1.** Annual statistical sensitivity of the muon EDM measurement of phase I and II.

$$a\vec{B} = \left(a - \frac{1}{\gamma^2 - 1}\right)\frac{\vec{\beta}\times\vec{E}}{c}, \tag{4}$$

with $|E| \approx a|B|c\beta\gamma^2$, which, in the nominal case of $\vec{B} \perp \beta$, results in $\vec{\omega}_a = 0$ and the spin is permanently aligned, i.e. frozen, to the momentum. Therefore, in the presence of an EDM one will observe a spin precession $\vec{\omega}_e \parallel \left(\vec{\beta}\times\vec{B}\right)$.

The frozen-spin technique benefits from a continuous build-up of the phase $\omega_e t$, and results in high statistical sensitivities. Two stages are considered at PSI. In the first phase (phase I) we will use surface muons with $p \approx 30\,\mathrm{MeV/c}$, while in the final setup (phase II) we would like to profit from the high flux available with $p = 125\,\mathrm{MeV/c}$ muons from pions decaying in flight. In a magnetic field of 3 T this results in an EDM sensitivity for a single muon of $\sigma(d_\mu) \approx 2 \times 10^{-17}\, e\cdot$cm and $\sigma(d_\mu) \approx 5 \times 10^{-17}\, e\cdot$cm, for a muon beam from decays of pions at rest and in flight, respectively. This, in turn, results in an electric field for the frozen-spin condition of $E_\mathrm{f} = 0.3\,\mathrm{MV/m}$ or $E_\mathrm{f} = 1.9\,\mathrm{MV/m}$.

In both phases we will inject the muons off-axis along the solenoid field direction. For a high injection rate, the muons need to pass through a dedicated collimation channel, which also includes a magnetic shield made of superconductors, as the acceptance phase space would be extremely small without the magnetic shield as a result of the magnetic mirror effect. The muons then spiral along the magnetic field to the center of the solenoid, where a quadrupole magnetic kick within the weakly focusing field region will twist the muon momentum onto a stable storage orbit. This longitudinal injection, also known as vertical injection, was first described in [22]. It profits from the advantage that the injection channel is far from the magnetically sensitive region of the storage zone and from a long delay, of the order of about 100 ns, between detecting a suitable muon using an entrance detector and the application of the magnetic kick. Table 1 summarizes all the

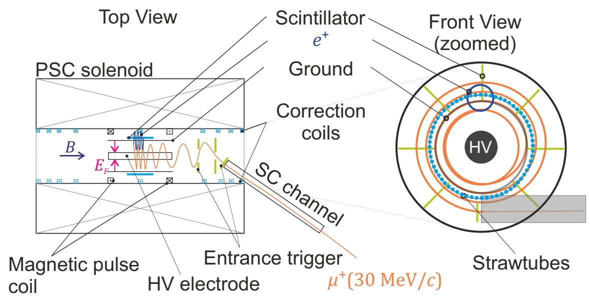


**Figure 2.** Side view (left) and front view (right) of the demonstrator experiment using an existing solenoid magnet with a field strength of 3 T.

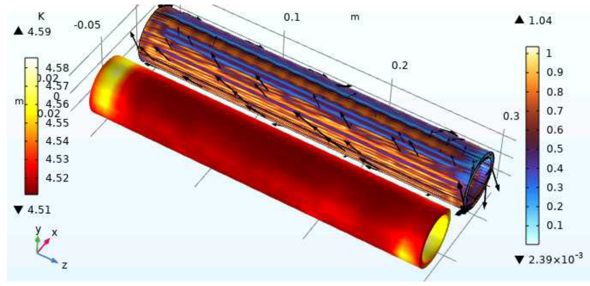

**Figure 3.** Finite element calculation of an injection tube made of a superconducting sheet.

factors necessary for the statistical sensitivity analysis in both phases.

## 3 Demonstration experiment using an existing solenoid

In the first phase, we intend to use an existing solenoid with a field of 3 T to demonstrate all the techniques necessary for the muon EDM search deploying the frozen-spin technique. A conceptual sketch is shown in Fig. 2. Muons with momentum of $P \approx 30\,\mathrm{MeV/c}$ from the decay of pions at rest with a polarization better than 95 % will be injected into a collimation tube of inner diameter ID= 15 mm and length $\ell \approx 800$ mm within a magnetic shield. While the collimation is the first step in reducing the phase space of the injected beam so as to match it to the tiny acceptance phase space, the magnetic superconducting shield (SC-channel) is essential to transport the muons from the low-field region at the exit of the beamline to the high-field region inside the solenoid. A set of correction coils will reduce the field gradient between the injection area at the exit of the collimation tube to increase the acceptance phase space. Once a muon is injected into the solenoid, a thin entrance scintillator in anticoincidence with a set of active apertures generates an entrance signal for muons within the acceptance phase space, which triggers a magnetic pulse in the center of the solenoid. The 100 ns short quadrupole magnetic pulse (pulse coil) twists the remaining longitudinal momentum, along the solenoid field, of the incident muon in the transverse direction. The muon is hence stored on a stable orbit inside the weakly-focusing field. An electric field $E_f = 3\,\mathrm{kV/cm}$ at the storage orbit is applied between two coaxial electrodes and establishes the frozen-spin technique. A combination of straw tubes and scintillating fiber mats track the decay positron to measure the $g-2$ frequency and the longitudinal asymmetry. The measurement of the $g-2$ frequency, $\omega_a$, will serve as a sensitive magnetic field probe. In addition, we will tune the $E$ field for the frozen-spin condition by measuring $\omega_a$ as a function of the applied electric field and interpolate to $\omega_a(E) = 0$.

## 4 Injection into the solenoid field

In a first step, we will demonstrate the off-axis injection into the solenoid and through a collimation channel inside a magnetic shield. In the fringe field of the solenoid magnet, below 1 T, we will use a thick iron tube as a magnetic shield. Above 1 T and up to 3 T a shield made of superconductor (SC) will be deployed. More than fifty years ago, Firth et al. demonstrated this for a 1.75 T bubble chamber at CERN [23] and it is used today, for example, in the BNL/FNAL (g-2) experiment [24]. The principal idea is that once the superconducting shield is cooled below the critical temperature $T_c$, ramping of the outside field will induce persistent currents inside the superconductor that counteract with the outside field. Therefore, the field inside the SC shield will remain as low as before the magnet was ramped. This effect persists if the shield is sufficiently thick and the mean lifetime of the shielding current is long enough. Once the field starts to penetrate, the outside field needs to be ramped down, and the superconducting shield can be reset by warming up above the critical temperature. We will test Nb-Ti/Nb/Cu sheets from the Wigner Research Center in Budapest, wound and clamped around a copper tube of ID=15 mm, and a design based on high-temperature superconducting ribbons / tapes wound helically onto a copper tube of the same diameter. Similar tests [25, 26] showed promising results for the Nb-Ti/Nb/Cu sheets, while the HTS ribbon design did not adequately shield against the outside field. We will investigate whether different mounting techniques and more layers of the helical wound HTS result in a sufficient shielding factor. This would be favorable as only liquid nitrogen temperature will be required if the final experiment's magnet also deploys HTS coils. We are currently preparing finite element models of superconducting shields (for illustration, see Fig.,3), and benchmark single layer models against physical prototypes (see Fig. 4). For the HTS shields, we are setting up a test facility using a liquid nitrogen bath and a Helmholtz coil. We will measure the shielding factor by taking the ratio of magnetic fields inside the tubes when the coil is ramped to the maximum field at room temperature and 70 K.

**Figure 4.** First prototype magnetic shields for the injection channel. On the left, two versions made of high temperature superconducting tape would onto a copper tube. On the right, two tube of standard iron tubes which might be used in the region with fields below 1 T.

## 5 Conclusion

At PSI we are setting up an experiment to search for the electric dipole moment of the muon using the frozen-spin technique. In the next few years, we will demonstrate essential experimental techniques using an existing solenoid magnet with a field strength of 3 T. For the injection of muons into the high-field region, we will deploy a SC shield made of either Nb-Ti/Nb/Cu sheets or HTS ribbon wound around a collimation tube. In this initial phase, we plan to demonstrate the frozen-spin technique by searching for muon EDM with a sensitivity of better than $3 \times 10^{-21}$ $e\cdot$cm using surface muons. In phase II, using an optimized highly uniform magnetic field and muons with a momentum of at least 125 MeV/c, we aim for a sensitivity of at least $6 \times 10^{-23}$ $e\cdot$cm.

## 6 Acknowledgments

The authors and the collaboration thank the excellent technical support of M. Meier from the UCN group and R. Deckardt and M. Duda from GFA at PSI. This work is partially financed by the Swiss National Science Fund's grant No.204118 and received funding from the Swiss State Secretariat for Education, Research and Innovation (SERI).

## References

[1] G. Lüders, Dan. Mat. Fys. Medd. **28**, 1 (1954)
[2] J.H. Smith, E.M. Purcell, N.F. Ramsey, Phys. Rev. **108**, 120 (1957)
[3] D. Berley, R.L. Garwin, G. Gidal, L.M. Lederman, Phys. Rev. Lett. **1**, 144 (1958)
[4] K. Jungmann, Ann. Phys. **525**, 550 (2013)
[5] T.E. Chupp, P. Fierlinger, M.J. Ramsey-Musolf, J.T. Singh, Rev. Mod. Phys. **91**, 015001 (2019)
[6] G.W. Bennett, B. Bousquet, H.N. Brown, G. Bunce, R.M. Carey, P. Cushman, G.T. Danby, P.T. Debevec, M. Deile, H. Deng et al. (Muon g-2), Phys. Rev. D **73**, 072003 (2006), `hep-ex/0602035`
[7] G.W. Bennett, B. Bousquet, H.N. Brown, G. Bunce, R.M. Carey, P. Cushman, G.T. Danby, P.T. Debevec, M. Deile, H. Deng et al. (Muon (g-2)), Phys. Rev. D **80**, 052008 (2009), `0811.1207`
[8] V. Andreev, D. Ang, D. DeMille, J. Doyle, G. Gabrielse, J. Haefner, N. Hutzler, Z. Lasner, C. Meisenhelder, B. O'Leary et al., Nature **562**, 355 (2018)
[9] J.N. Butler, arXiv e-prints arXiv:1709.03006 (2017), `1709.03006`
[10] L. Masetti, A. Collaboration, Nuclear and Particle Physics Proceedings **303-305**, 43 (2018)
[11] M. Raidal, A. Schaaf, I. Bigi, M. Mangano, Y. Semertzidis, S. Abel, S. Albino, S. Antusch, E. Arganda, B. Bajc et al., Eur. Phys. J. C **57**, 13 (2008), `0801.1826`
[12] B. Capdevila, A. Crivellin, S. Descotes-Genon, J. Matias, J. Virto, JHEP **2018**, 93 (2018), `1704.05340`
[13] W. Altmannshofer, P. Stangl, Eur. Phys. J. C **81**, 952 (2021), `2103.13370`
[14] LHCb Collaboration, R. Aaij, C. Abellán Beteta, T. Ackernley, B. Adeva, M. Adinolfi, H. Afsharnia, C.A. Aidala, S. Aiola, Z. Ajaltouni et al., Nature Physics **18**, 277 (2022), `2103.11769`
[15] T. Aoyama, N. Asmussen, M. Benayoun, J. Bijnens, T. Blum, M. Bruno, I. Caprini, C.M. Carloni Calame, M. Cè, G. Colangelo et al., Phys. Rep. **887**, 1 (2020), `2006.04822`
[16] B. Abi, T. Albahri, S. Al-Kilani, D. Allspach, L.P. Alonzi, A. Anastasi, A. Anisenkov, F. Azfar, K. Badgley, S. Baeßler et al. (Muon $g-2$ Collaboration), Phys. Rev. Lett. **126**, 141801 (2021)
[17] V. Cirigliano, B. Grinstein, G. Isidori, M.B. Wise, Nuclear Physics B **728**, 121 (2005), `hep-ph/0507001`
[18] J.L. Feng, K.T. Matchev, Y. Shadmi, Nucl. Phys. **B613**, 366 (2001), `hep-ph/0107182`
[19] A. Crivellin, M. Hoferichter, P. Schmidt-Wellenburg, Phys. Rev. D **98**, 113002 (2018), `1807.11484`
[20] L. Thomas, The London, Edinburgh, and Dublin Philosophical Magazine and Journal of Science **3**, 1 (1927)
[21] V. Bargmann, L. Michel, V.L. Telegdi, Phys. Rev. Lett. **2**, 435 (1959)
[22] H. Iinuma, H. Nakayama, K. Oide, K.i. Sasaki, N. Saito, T. Mibe, M. Abe, Nucl. Instr. Meth. Phys. Res. A **832**, 51 (2016)
[23] M. Firth, E. Habel, L. Krempasky, F. Schmeissner, Conf. Proc. C **730508**, 79 (1973)
[24] A. Yamamoto, Y. Makida, K. Tanaka, F. Krienen, B. Roberts, H. Brown, G. Bunce, G. Danby, M. G-

Perdekamp, H. Hseuh et al., Nuclear Instruments and Methods in Physics Research Section A: Accelerators, Spectrometers, Detectors and Associated Equipment **491**, 23 (2002)

[25] D. Barna, Phys. Rev. Accel. Beams **20**, 041002 (2017)

[26] D. Barna, M. Novák, K. Brunner, C. Petrone, M. Atanasov, J. Feuvrier, M. Pascal, IEEE Trans. Appl. Supercond. **29**, 4900108 (2018), 1809.04330